International Journal of Engineering

Journal Homepage: www.ije.ir

TECHNICAL NOTE

Evaluation of Seismic Response of Concrete Structures Reinforced by Shape Memory Alloys

H. Jahangir[a], M. Bagheri*[b]

[a] *Department of Civil Engineering, Ferdowsi University of Mashhad, Mashhad, Iran*
[b] *Department of Civil Engineering, Birjand University of Technology, Birjand, Iran*

PAPER INFO

Paper history:
Received 30 November 2019
Received in revised form 22 December 2019
Accepted 17 Januray 2020

Keywords:
Maintenance Costs
Plastic Hinge Length
Reinforced Concrete Structures
Shape Memory Alloys
Time History Analysis

ABSTRACT

Shape memory alloys (SMAs) are unique smart materials that have many advantages, such as ability to resist large strains without leaving residual strains and ability to recover original form. However, the high costs of SMAs have limited their usage. This paper evaluates the behavior of concrete structures equipped with SMAs in an optimal manner as they are being used along with plastic hinge of the beams. For this purpose, a reinforced concrete (RC) beam, a 2D RC frame and a 3D RC building were considered, which were tested in previous studies under cyclic loading and on a shaking table. After verifying RC beam in the Seismostruct software, the steel rebars are replaced by SMAs in all connections of models and time history analysis is performed. The seismic response of concrete structures equipped with SMAs is compared with the conventional RC structures. The maximum base shear and roof displacement, amount of residual displacement and distribution of interstory drift at the structure height are among the factors to be evaluated. The results showed that, due to the use of SMAs in concrete structures, the maximum base shear did not significantly change compared with the conventional RC structures, and the residual displacements in the structure roof have been reduced. On the other hand, the maximum displacement of the roof was increased in the structures with SMAs. The concrete structures equipped with SMAs experience a slight residual deformation, and the distribution of interstory drift is even more uniform at the height of such structures.

***doi**: 10.5829/ije.2020.33.03c.05*

1. INTRODUCTION

Structures in the areas with high seismic hazard are severely damaged by strong earthquakes. In the reinforced concrete (RC) structures, the damages mostly occur in the plastic hinge of the beams and cause residual displacements in the structure [1]. Although, the RC buildings may resist strong earthquakes, the resulting residual displacements increase the repair and reconstruction costs and greatly reduce the resistant of structures to the aftershocks [2]. To solve this problem, methods such as the reinforcement of structural elements using the fiber reinforced polymer (FRP) [3,4] and fiber reinforced inorganic matrix (FRIM) composites can be utilized [5–7]. But, using the shape memory alloys with the self-centering feature can be a more appropriate solution.

Shape memory alloys (SMAs) are new smart materials that can resist large nonlinear deformations and return back to the original geometry after unloading which made them an appropriate choice for reducing the maintenance costs [8]. In the past decades, many researchers have evaluated the possibility of using SMAs for the structural applications such as dampers [9–11], reinforcements [12–17], bracing [18,19], seismic isolation systems [20–22] and actuators [23,24].

Although previous studies have shown that the use of SMAs can reduce the residual displacements in the RC structures [25–27], their operating costs is one of challenges for using the alloys in the RC structures. One of the strategies to reduce the cost of these alloys is to use them only in the sections that experience more deformation due to the applied loads. The plastic hinges of beams are one of the sections evaluated in this paper.

*Corresponding Author Email: *mnsrbagheri@birjandut.ac.ir* (M. Bagheri)

Please cite this article as: H. Jahangir, M. Bagheri, Evaluation of Seismic Response of Concrete Structures Reinforced by Shape Memory Alloys, International Journal of Engineering (IJE), IJE TRANSACTIONS C: Aspects Vol. 33, No. 3, (March 2020) 410-418

In this paper, the effect of individual SMA features on improving seismic behavior of RC structures was evaluated. SMAs are optimally used as an alternative to steel rebar in the plastic hinges of beams. Three laboratory full scale RC structures, a RC beam, a frame and a building, were selected for the modeling. After being assured of numerical model of RC beam and replacing the SMAs in the plastic hinges of frame and building beams, the time history analysis is performed. The base shear, maximum roof displacement, residual displacements and distribution of drift are among the factors that are evaluated in the RC structures equipped with the SMAs, and their seismic response is compared with the conventional RC structures equipped by steel rebars.

2. SHAPE MEMORY ALLOYS

Shape memory alloys are known as one of smart and innovative materials which have unique advantages such as ability to resist high strains without leaving residual strains, high resistance to corrosion and fatigue, ability to recover original shape and high energy dissipation [28]. SMAs have two crystalline phases, austenite and martensite. Austenite is stable at high temperatures and low stresses and martensite at low temperatures and high stresses [29]. The transformation of austenitic to martensitic phases and, consequently, the shape memory and superelasticity features of the SMAs have led researchers to use these smart materials in various areas.

In this paper, the superelasticity feature of SMAs are used to improve the seismic behavior of RC structures. For this purpose, the stress-strain model of these alloys is used, which is introduced by Auricchio and Sacco [30] and also used in SeismoStruct finite element software [31] as illustrated in Figure 1.

The governing parameters in the model are σ_f^{EA} (stresses related to the start of the austenitic phase transformation into the martensitic phase), σ_s^{SA} (stresses related to the end of the austenitic phase transformation into the martensitic phase), σ_s^{AS} (stresses related to the start of the unloading step), σ_f^{AS} (stresses related to the end of the unloading step), ε_l (equivalent strain in the unloading step), and E_{SMA} (elastic modulus in the austenitic phase) [30].

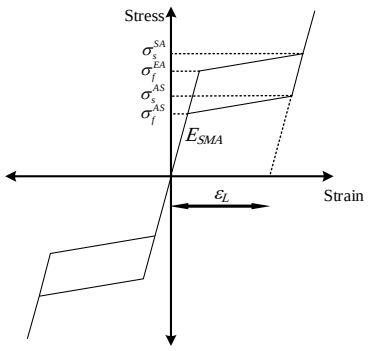

Figure 1. SMA stress-strain model [30]

3. NUMERICAL MODES

In this work, three laboratory structures of a RC beam [32], a 2D concrete frame [33] and a 3D RC building [34], the behavior of which was evaluated in the previous studies under cyclic loading and on the shaking table, was used for numerical modeling in SeismoStruct finite element software [31].

3. 1. Model Verification Figure 2 shows geometrical properties of selected RC beam [32] which was tested under cyclic loading including six cycles applied as the beam rotation angle (R = θ_1+ θ_2) reached to 0.125, 0.25, 0.50, 1.0, 1.5 and 2.0%. The concrete, steel and SMA material characteristics used in the construction of RC beam model are reported in Tables 1 and 2, respectively.

As shown in Figure 3, the numerical model of RC beam was constructed in SeismoStruct finite element software [31].

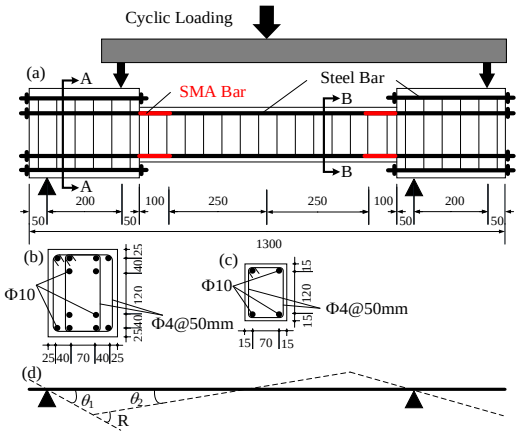

Figure 2. a) Test set-up; b) beam section (A-A); c) beam section (B-B) and d) deformed shape (dimensions in mm)

TABLE 1. Mechanical properties of materials

Materials	Features	RC beam	2D frame	3D building
Concrete	Compressive strength (MPa)	34	25	35
	Tensile strength (MPa)	2.96	2.7	3.4
	Ultimate strain (%)	0.31	0.3	0.35
Steel	Modulus of elasticity (MPa)	186,000	200,000	200,000
	Yield stress (MPa)	362.9	235	385
	Strain hardening ratio (%)	0.5	0.5	0.6

TABLE 2. Mechanical properties of SMAs

Feature	RC beam	2D frame and 3D building
σ_f^{EA} (MPa)	203.9	320
σ_s^{SA} (MPa)	224.6	460
σ_s^{AS} (MPa)	211.3	260
σ_f^{AS} (MPa)	187.4	190
E_{SMA} (MPa)	30,000	28,000
ε_l (%)	4.13	4.25

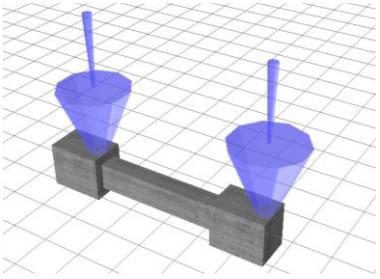

Figure 3. Numerical model of RC beam

For the concrete materials, the nonlinear stress-strain relationship was used based on Mander et al. [35] model. The steel materials were modeled by bilinear stress-strain relationship. The section of elements was divided into 400 fibers, and the 6 integration points were used to obtain the stresses and strains in each of the fibers. Figure 4 shows the comparison of the hysteretic curves obtained from the numerical analysis and the reported experimental test.

As shown in Figure 4, there is a good agreement between the experimental and numerical results of RC beam and SeismoStruct software can be safely used to model the 2D frame and 3D building.

3. 2. 2D Frame and 3D Building Models The geometrical properties of considered 2D RC frame [33] is shown in Figure 5. The combination of dead and live load is equal to 15.1 kN/m for the 1st to 3th stories and 12.7 kN/m for the roof. The characteristics of concrete and steel materials used in the construction of this concrete frame are reported in Table 1 [33].

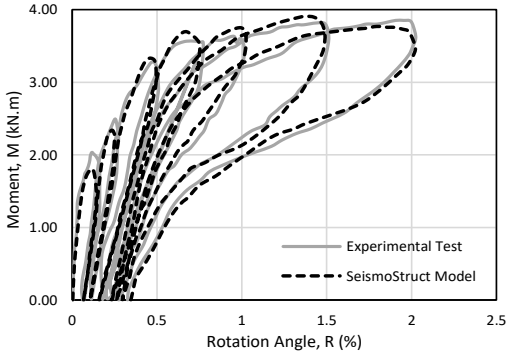

Figure 4. Maximum moment - rotation angle curves in experimental test [32] and numerical analysis

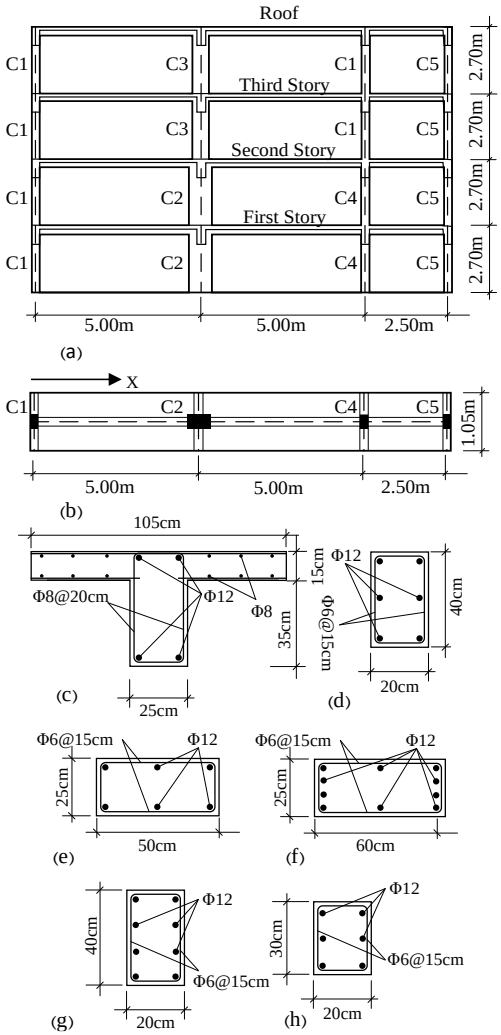

Figure 5. a) Elevation view; b) plan view; c) T-shape beam section, and sections of column: d) C1; e) C2; f) C3; g) C4; and h) C5 in laboratory concrete frame

The geometric properties of selected three-story concrete building with the moment-resisting frames [34] are shown in Figure 6.

Figure 7 shows the section of the elements constituting the reinforced concrete building. The mechanical properties of the materials used in the construction of the concrete model are reported in Table 1. The gravity dead and live loads of this model were 0.5 and 2.0 kN/m^2, respectively.

The SMA rebars replaced the steel ones in the location of beam plastic hinges in order to evaluate the efficiency of the alloys. The relation proposed by Paulay and Preiestley [36] was used to calculate the length of the beam plastic hinge:

$$0.08z + 0.022d_b f_y \quad (1)$$

In Equation (1), z is the distance between the beam-to-column joints and the point where the sign of bending moment diagram changes along the beam, which is $0.2113l$ (l = beam length). d_b and f_y are the sum of the longitudinal rebar diameters (m) and the steel yield stress (MPa), respectively [36]. Table 3 shows the plastic hinges calculated by Equation (1) in the 2D frame and 3D building model beams.

The mechanical properties of SMAs introduced into SesimoStruct software using the stress-strain relationship proposed by Auricchio and Sacco [30] are reported in Table 3. Figure 8 shows the constructed models of 2D frame and 3D building in SesimoStruct software.

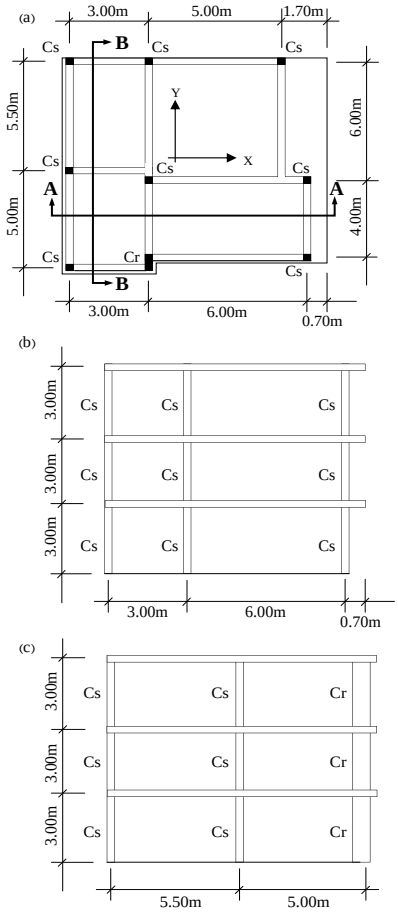

Figure 6. a) Plan view; b) elevation view (section A-A); c) elevation view (section B-B) of 3D concrete building

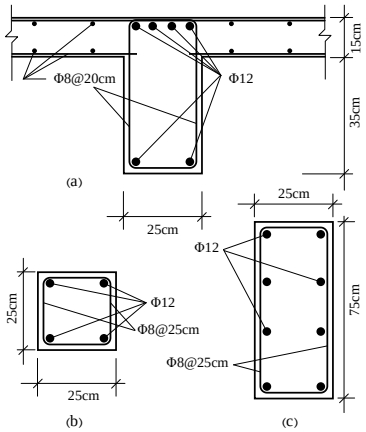

Figure 7. 3D building element sections a) typical T-shaped beam; b) C_s and c) C_r

4. TIME HISTORY ANALYSIS

According to Table 4, the widely recognized accelerograms are selected and scaled based on the design response spectrum of 0.3g intensity for type III

TABLE 3. Length of beam plastic hinges in models

Model	beam length (m)	plastic hinges length (m)
2D Frame	2.5	0.29
	5.0	0.33
3D Building	3.0	0.66
	4.0	0.68
	5.0	0.69
	5.5	0.71
	6.0	0.72

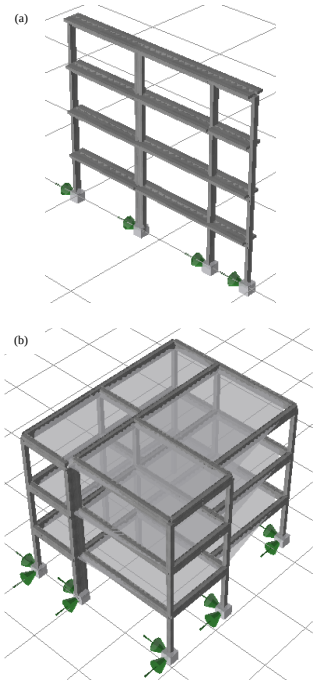

Figure 8. a) 2D frame and b) 3D building models in SesimoStruct software

soil with the 5% damping (B_D3_0.3g) to conduct the time history analysis in this paper. The spectral acceleration (SA) of scaled accelerograms along with the mean values are shown in Figure 9. As an instance, Figure 10 shows the hysteretic curves of models resulted from Friuli loaded accelerogram.

In the following section, maximum base shear, maximum roof displacement, residual displacement of roof, and distribution of interstory drifts in the height of models were evaluated to realize the performance of SMAs.

4. 1. Maximum Base Shear Figure 11 shows the maximum base shear in the 2D frame model and 3D building in the X and Y directions in two cases, reinforced with steel rebar (STEEL) and equipped with SMAs (SMA) along with the mean values in each case. Figure 11a shows that in most cases in 2D frame model, the maximum base shear is higher in the models equipped with the SMAs than those reinforced with steel rebar. Figures 11b and 11c show that the maximum base shear in the 3D building model in the both X and Y directions is higher for STEEL reinforced case than SMA equipped one. The maximum base shear value in the both cases in the Y direction is greater than the X direction, which indicates that the model stiffness in the Y direction is greater than that in the X direction.

TABLE 4. Selected accelerograms for time history analysis

No.	Event Name	Magnitude (Richter)	Peak acceleration (g)
1	Elcentro	6.9	0.334
2	Friuli	6.5	0.498
3	Hollister	5.6	0.338
4	Imperial_Valley	6.5	0.293
5	Kobe	6.9	0.317
6	Kocaeli	7.5	0.346
7	Loma-Prieta	6.8	0.397
8	Northridge	6.7	0.434

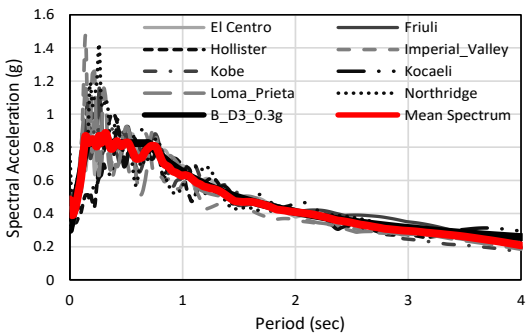

Figure 9. Spectral acceleration of scaled accelerograms for time history analysis

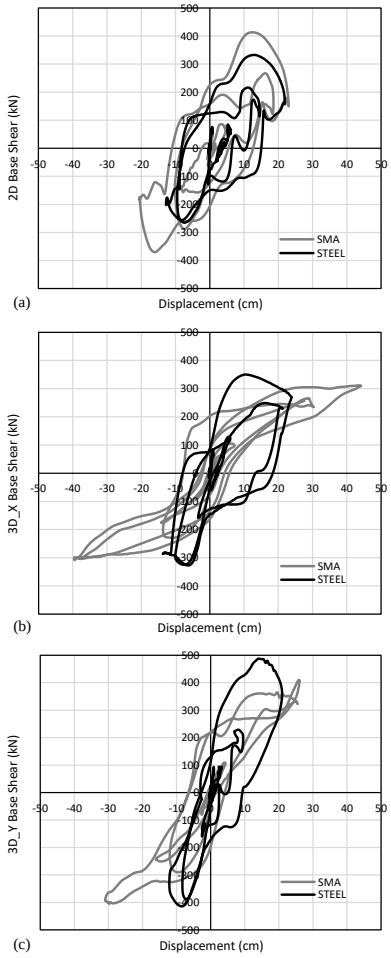

Figure 10. Hysteresis curves form Friuli loaded accelerogram analysis: a) 2D frame; b) 3D building (X direction); c) 3D building (Y direction)

In general, it can be stated that the use of SMAs as a substitute for steel rebar in the location of beam plastic hinges in a 2D frame model resulted in an increase in the maximum base shear, and in a 3D building model, it reduces the shear. It should be noted that the difference in the maximum base shear between the two SMA equipped and STEEL reinforced cases, relative to the highest value in the 2D frame model is 13.4% and in the 3D building model in the X and Y direction are 10.4 and 10.9%, respectively. Therefore, the maximum base shear could be considered the same in the both cases.

4. 2. Maximum Roof Displacement Figure 12 shows the maximum displacement of roof in models. Figure 12a shows that by applying most earthquakes (except Kocaeli) on 2D frame model, the maximum roof displacement in the SMA equipped case is higher than STEEL reinforced one. Figures 12b and 12c showed that in 3D building model, the maximum roof displacement in SMA equipped models is more than STEEL reinforced

ones. The application of Friuli and Northridge earthquakes in the X direction and the Friuli, Hollister and Kobe earthquakes in the Y direction caused the greatest difference between the maximum roof displacement in the two cases.

The higher displacement in SMA equipped models than that in STEEL reinforced ones shows that SMAs increases the ductility of the models. The results of maximum base shear and roof displacement indicate that use of SMAs, while keeping the base shear constant and increasing the displacements, causes the dissipation of earthquake energy as deformation prevents the stress increase in the elements.

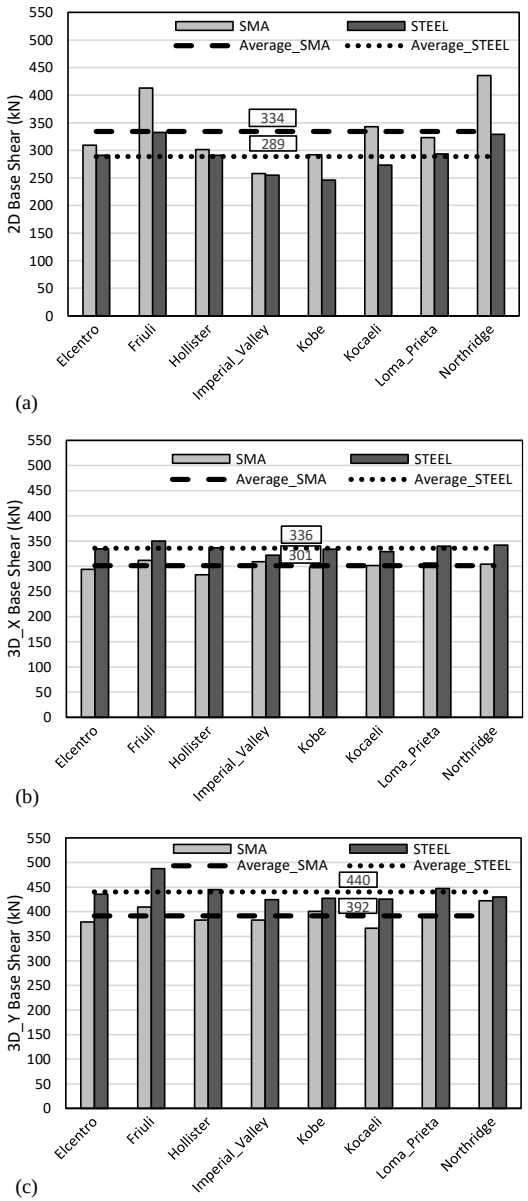

Figure 11. Maximum base shear: a) 2D frame; b) 3D building (X direction); c) 3D building (Y direction)

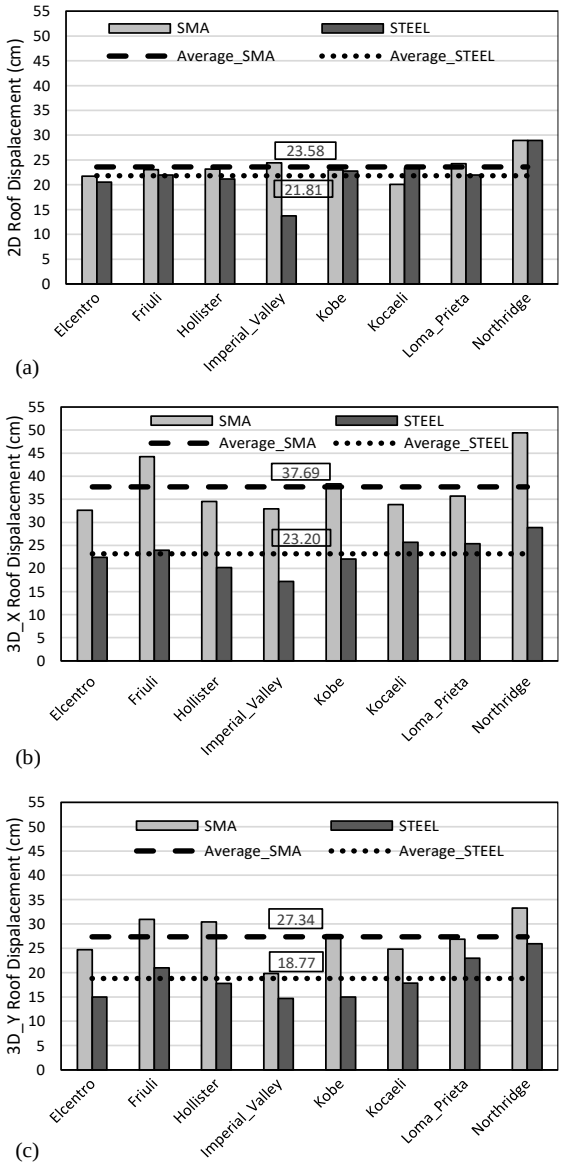

Figure 12. Maximum roof displacement: a) 2D frame; b) 3D building (X direction); c) 3D building (Y direction)

4. 3. Residual Roof Displacement Figure 13 shows the amount of residual roof displacement in 2D frame and 3D building models. Figures 13a, 13b and 13c show that in all earthquakes, the amount of residual displacement in the roof of SMA equipped models is greatly reduced compared with STEEL reinforced ones. Therefore, it can be stated with full confidence that the use of SMAs will greatly help to reduce the incurred damages and the repair costs after the end of the earthquake in the reinforced concrete models.

4. 4. Interstory Drift Distribution Figure 14 shows the distribution of maximum interstory drifts at the height of the 2D frame and 3D building models.

Figure 14 shows that in the both STEEL reinforced models, the maximum interstory drift is related to the first floor of the model and is reduced in the higher floors. Hence, the maximum interstory drifts are not uniformly distributed at the height, and there is the possibility of soft floor in the first floor of the models. In SMA equipped models, a more uniform distribution of the interstory drifts is resulted. As a result, SMAs prevent the formation of soft floor and its corresponding sudden failures in structures.

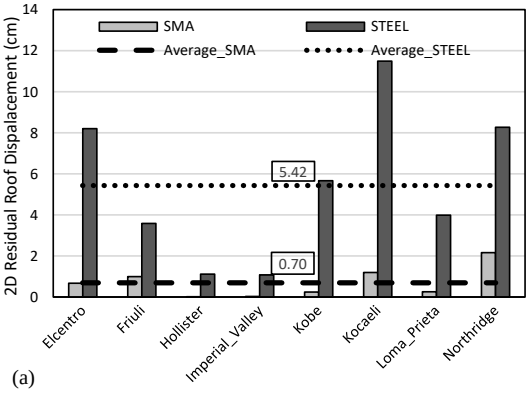

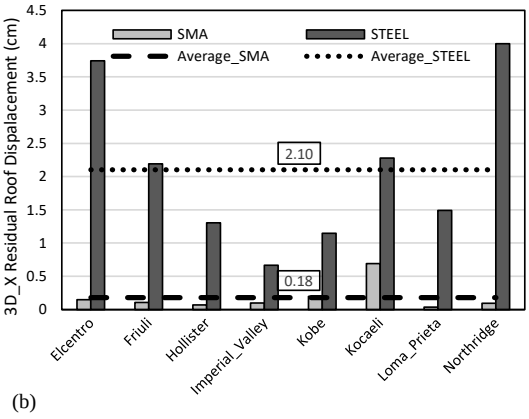

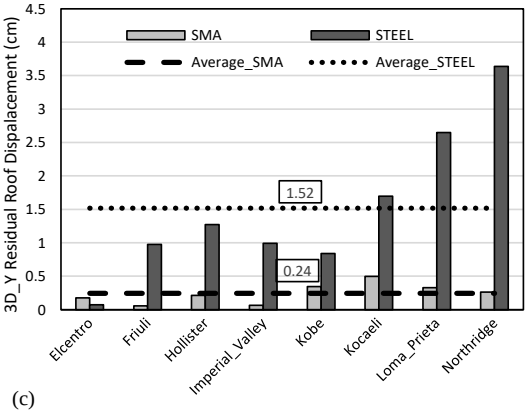

Figure 13. Residual roof displacement: a) 2D frame; b) 3D building (X direction); c) 3D building (Y direction)

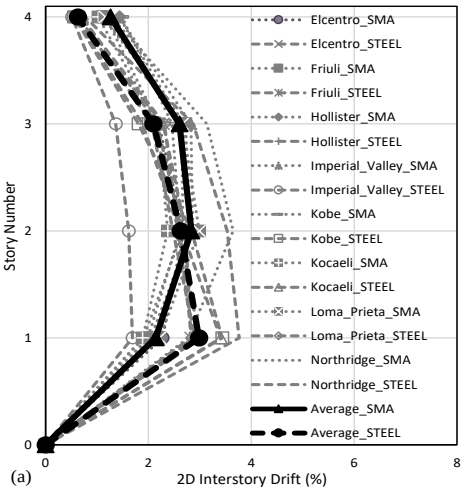

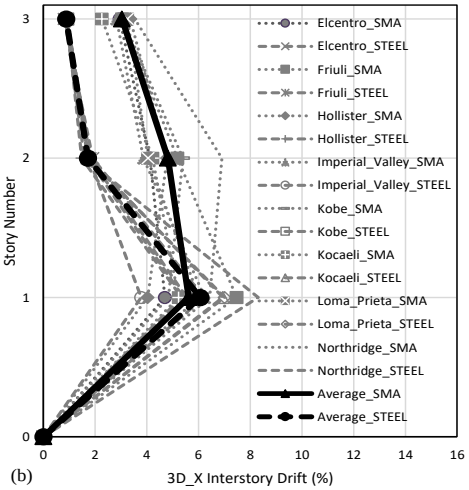

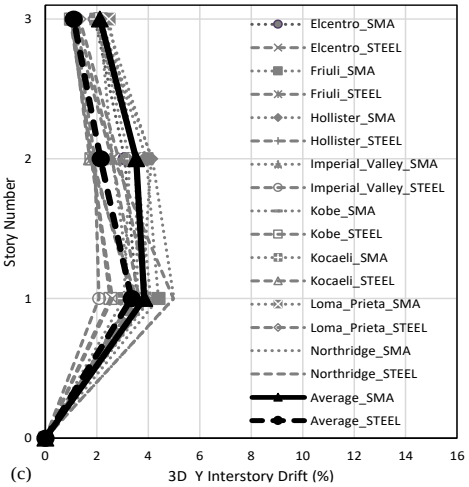

Figure 14. Distribution of interstory drifts: a) 2D frame; b) 3D building (X direction); c) 3D building (Y direction)

5. COST ANALYSIS

Cost investigations showed that average price of different SMAs decreased from US$1100/kg in 1999 to around

US$24/kg in 2019. Based on the calculated plastic hinges reported in Table 3, the cost of 2D frame and 3D building models equipped with SMA rebars is 14.32 and 19.71% more than the conventional steel reinforced models, respectively. However, using SMA could significantly decrease repair costs, which recover such an increase in construction costs.

6. CONCLUSION

This paper evaluated the effect of shape memory alloys on improving seismic behavior of numerical models generated based on experimental 2D RC frame and 3D building, through their application along the plastic hinge of the beams. By analyzing the time history for the models, parameters such as maximum base shear, maximum roof displacement, residual displacement, and interstory drift were evaluated. The results of the analyses can be summarized as follows:

1) The difference in the maximum base shear between SMA equipped and STEEL reinforced cases, relative to the highest value in the 2D frame model is 13.4% and in the 3D building model in the X and Y directions are 10.4 and 10.9%, respectively, and hence, the maximum base shear in these two cases can be considered the same.

2) The difference in the maximum roof displacement between SMA equipped and STEEL reinforced cases, relative to the highest value in the 2D frame model is equal to 7.5%, and in the 3D building model in the X and Y directions are equal to 38.4 and 31.3%, respectively. Therefore, it can be concluded that the use of SMAs, while keeping the base shear constant and increasing the displacement, causes the dissipation of earthquake energy in the form of deformation in the concrete models and prevents the stress increase in the elements.

3) The amount of reduction in the residual roof displacement in SMA equipped case compared to STEEL reinforced one, relative to the highest value in the 2D frame model is equal to 87.1%, and in the 3D building model in the X and Y directions are 91.4 and 84.2%, respectively. Consequently, it can be stated that the use of SMAs will help to reduce the damages and the maintenance costs.

4) The analyses show that the use of SMAs results in a more uniform distribution of the interstory drifts in the height of the structure and, as a result, prevents the formation of soft floor and the sudden failure in the structure.

7. REFERENCES

1. Ho, J. C. M., Lam, J. Y. K., and Kwan, A. K. H., "Effectiveness of adding confinement for ductility improvement of high-strength concrete columns", ***Engineering Structures***, Vol. 32, No. 3, (2010), 714–725.
2. Comartin, C. D., Greene, M., and Tubbesing, S. K., "The Hyogoken Nanbu Earthquake: Great Hanshin Earthquake Disaster", Preliminary Reconnaissance Report, (1995).
3. Kianoush, M. and Esfahani, M. R., "Axial Compressive Strength of Reinforced Concrete Columns Wrapped with Fiber Reinforced Polymers (FRP).", ***International Journal of Engineering, Transactions B: Applications***, Vol. 18, No. 1, (2005), 9–19.
4. Bagheri, M., Chahkandi, A., and Jahangir, H., "Seismic Reliability Analysis of RC Frames Rehabilitated by Glass Fiber-Reinforced Polymers", ***International Journal of Civil Engineering***, Vol. 17, No. 11, (2019), 1785–1797.
5. Jahangir, H. and Esfahani, M. R., "Numerical Study of Bond – Slip Mechanism in Advanced Externally Bonded Strengthening Composites", ***KSCE Journal of Civil Engineering***, Vol. 22, No. 11, (2018), 4509–4518.
6. Santandrea, M., Imohamed, I. A. O., Jahangir, H., Carloni, C., Mazzotti, C., De Miranda, S., Ubertini, F., and Casadei, P., "An investigation of the debonding mechanism in steel FRP- and FRCM-concrete joints", In 4th Workshop on the new boundaries of structural concrete, (2016), 289–298.
7. Jahangir, H. and Esfahani, M., "Strain of newly – developed composites relationship in flexural tests", ***Journal of Structural and Construction Engineering***, Vol. 5, No. 3, (2018), 92–107.
8. Asgarian, B. and Moradi, S., "Seismic response of steel braced frames with shape memory alloy braces", ***Journal of Constructional Steel Research***, Vol. 67, No. 1, (2011), 65–74.
9. Dolce, M., Cardone, D., and Ponzo, F. C., "Shaking-table tests on reinforced concrete frames with different isolation systems", ***Earthquake Engineering & Structural Dynamics***, Vol. 36, No. 5, (2007), 573–596.
10. Qian, H., Li, H., and Song, G., "Experimental investigations of building structure with a superelastic shape memory alloy friction damper subject to seismic loads", ***Smart Materials and Structures***, Vol. 25, No. 12, (2016), 125026-125040.
11. Dutta, S. C. and Majumder, R., "Shape Memory Alloy (SMA) as a Potential Damper in Structural Vibration Control", In Advances in Manufacturing Engineering and Materials, (2019), 485–492.
12. Saiidi, M. S. and Wang, H., "Exploratory study of seismic response of concrete columns with shape memory alloys reinforcement", ***ACI Materials Journal***, Vol. 103, No. 3, (2006), 436–443.
13. Youssef, M. A., Alam, M. S., and Nehdi, M., "Experimental Investigation on the Seismic Behavior of Beam-Column Joints Reinforced with Superelastic Shape Memory Alloys", ***Journal of Earthquake Engineering***, Vol. 12, No. 7, (2008), 1205–1222.
14. Abdulridha, A., Palermo, D., Foo, S., and Vecchio, F. J., "Behavior and modeling of superelastic shape memory alloy reinforced concrete beams", ***Engineering Structures***, Vol. 49, (2013), 893–904.
15. Malagisi, S., Marfia, S., Sacco, E., and Toti, J., "Modeling of smart concrete beams with shape memory alloy actuators", ***Engineering Structures***, Vol. 75, (2014), 63–72.
16. Moon, D. Y., Roh, H., and Cimellaro, G. P., "Seismic Performance of Segmental Rocking Columns Connected with NiTi Martensitic SMA Bars", ***Advances in Structural Engineering***, Vol. 18, No. 4, (2015), 571–584.
17. Shahverdi, M., Michels, J., Czaderski, C., and Motavalli, M., "Iron-based shape memory alloy strips for strengthening RC members: Material behavior and characterization", ***Construction and Building Materials***, Vol. 173, (2018), 586–599.
18. Gao, N., Jeon, J.-S., Hodgson, D. E., and DesRoches, R., "An innovative seismic bracing system based on a superelastic shape memory alloy ring", ***Smart Materials and Structures***, Vol. 25, No. 5, (2016), 055030–055046.
19. Qiu, C. and Du, X., "Seismic performance of multistory CBFs with novel recentering energy dissipative braces", ***Journal of Constructional Steel Research***, (2019), 105864. https://doi.org/10.1016/j.jcsr.2019.105864.

20. Jalali, A., Cardone, D., and Narjabadifam, P., "Smart restorable sliding base isolation system", ***Bulletin of Earthquake Engineering***, Vol. 9, No. 2, (2011), 657–673.
21. Mishra, S. K., Gur, S., Roy, K., and Chakraborty, S., "Response of Bridges Isolated by Shape Memory–Alloy Rubber Bearing", ***Journal of Bridge Engineering***, Vol. 21, No. 3, (2016), 04015071–04015086.
22. Hedayati Dezfuli, F. and Alam, M. S., "Smart Lead Rubber Bearings Equipped with Ferrous Shape Memory Alloy Wires for Seismically Isolating Highway Bridges", ***Journal of Earthquake Engineering***, Vol. 22, No. 6, (2018), 1042–1067.
23. Sayyaadi, H. and Zakerzadeh, M. R., "Nonlinear Analysis of a Flexible Beam Actuated by a Couple of Active SMA Wire Actuators", ***International Journal of Engineering, Transactions C: Aspects***, Vol. 25, No. 3, (2012), 249–264.
24. Mir Mohammad Sadeghi, S. A., Hoseini, S. F., Fathi, A., and Mohammadi Daniali, H., "Experimental Hysteresis Identification and Micro-position Control of a Shape-Memory-Alloy Rod Actuator", ***International Journal of Engineering, Transactions A: Basics***, Vol. 32, No. 1, (2019), 71–77.
25. Alam, M. S., Youssef, M. A., and Nehdi, M., "Analytical prediction of the seismic behaviour of superelastic shape memory alloy reinforced concrete elements", ***Engineering Structures***, Vol. 30, No. 12, (2008), 3399–3411.
26. Alam, M. S., Youssef, M. A., and Nehdi, M. L., "Exploratory investigation on mechanical anchors for connecting SMA bars to steel or FRP bars", ***Materials and Structures***, Vol. 43, No. 1, (2010), 91–107.
27. Muntasir Billah, A. H. M. and Shahria Alam, M., "Seismic performance of concrete columns reinforced with hybrid shape memory alloy (SMA) and fiber reinforced polymer (FRP) bars", ***Construction and Building Materials***, Vol. 28, No. 1, (2012), 730–742.
28. DesRoches, R., McCormick, J., and Delemont, M., "Cyclic Properties of Superelastic Shape Memory Alloy Wires and Bars", ***Journal of Structural Engineering***, Vol. 130, No. 1, (2004), 38–46.
29. Malécot, P., Lexcellent, C., Folte^te, E., and Collet, M., "Shape Memory Alloys Cyclic Behavior: Experimental Study and Modeling", ***Journal of Engineering Materials and Technology***, Vol 128, No. 3, (2006), 335–345.
30. Auricchio, F. and Sacco, E., "A Superelastic Shape-Memory-Alloy Beam Model", ***Journal of Intelligent Material Systems and Structures***, Vol. 8, No. 6, (1997), 489–501.
31. Seismosoft, "SeismoStruct v7.0 - A computer program for static and dynamic nonlinear analysis of framed structures", Pavia, Italy. Seismic Support Service, (2014).
32. Pareek, S., Suzuki, Y., Araki, Y., Youssef, M. A., and Meshaly, M., "Plastic hinge relocation in reinforced concrete beams using Cu-Al-Mn SMA bars", ***Engineering Structures***, Vol. 175, (2018), 765–775.
33. Zendaoui, A., Kadid, A., and Yahiaoui, D., "Comparison of Different Numerical Models of RC Elements for Predicting the Seismic Performance of Structures", ***International Journal of Concrete Structures and Materials***, Vol. 10, No 4, (2016), 461–478.
34. Negro, P. and Mola, E., "A performance based approach for the seismic assessment and rehabilitation of existing RC buildings", ***Bulletin of Earthquake Engineering***, Vol. 15, No. 8, (2017), 3349–3364.
35. Mander, J. B., Priestley, M. J. N., and Park, R., "Theoretical Stress-Strain Model for Confined Concrete", ***Journal of Structural Engineering***, Vol 114, No. 8, (1988), 1804–1826.
36. Paulay, T. and Priestley, M. J. N., "Seismic Design of Reinforced Concrete and Masonry Buildings", Wiley – Interscience, (1992).

Evaluation of Seismic Response of Concrete Structures Reinforced by Shape Memory Alloys

TECHNICAL NOTE

H. Jahangir[a], M. Bagheri[b]

[a] *Department of Civil Engineering, Ferdowsi University of Mashhad, Mashhad, Iran*
[b] *Department of Civil Engineering, Birjand University of Technology, Birjand, Iran*

PAPER INFO

Paper history:
Received 30 November 2019
Received in revised form 22 December 2019
Accepted 17 Januray 2020

Keywords:
Maintenance Costs
Plastic Hinge Length
Reinforced Concrete Structures
Shape Memory Alloys
Time History Analysis

چکیده

آلیاژهای حافظه‌دار شکلی، مصالح هوشمند منحصر به فردی هستند که دارای برتری‌های مانند توانایی تحمل کرنش‌های زیاد بدون باقی‌ماندن کرنش‌های پس‌ماند و توانایی برگشت به شکل نخستین می‌باشند. اگرچه، هزینه‌های بالای این مصالح محدودیت‌هایی را در به‌کارگیری آن‌ها را ایجاد کرده است. این مقاله به ارزیابی رفتار ساختمان‌ها بتنی مجهز به این آلیاژها به‌صورت بهینه و با به‌کارگیری آن‌ها در طول مفصل پلاستیک تیرها پرداخته است. برای این منظور، از یک تیر بتن‌آرمه، قاب و ساختمان بتن‌آرمه‌ای که در پژوهش‌های پیشین تحت بار رفت و برگشتی و روی میز لرزه آزمایش شده‌اند، استفاده شده است. پس از راست‌آزمایی نمونه تیر بتن‌آرمه در نرم‌افزار، در اتصال‌های قاب و ساختمان بتن‌آرمه آلیاژهای حافظه‌دار شکلی جایگزین میلگردهای فولادی شد. رفتار لرزه‌ای سازه‌های بتنی مجهز به آلیاژها با سازه‌های بتن‌آرمه‌ی معمولی مقایسه شدند. بیشینه برش پایه و جابجایی بام، مقدار جابجایی پس‌ماند و چگونگی توزیع دریفت بین طبقه‌ای در ارتفاع سازه از عامل‌های مورد ارزیابی هستند. نتیجه‌ها نشان می‌دهند که در اثر استفاده از آلیاژهای حافظه‌دار شکلی، بیشینه برش پایه نسبت به سازه‌های بتن‌آرمه‌ی معمولی تغییر چندانی نمی‌کند، جابجایی‌های پس‌ماند در بام سازه کاهش می‌یابندو بیشینه جابجایی بام بیشتر شده است. در پایان زلزله نیز، توزیع دریفت‌های بین طبقه‌ای نیز در در ارتفاع یکنواخت‌تر است.

***doi**: 10.5829/ije.2020.33.03c.05*